

Thermal Management of Pouch Cell under Extreme Climate Conditions Using T-Shaped Cold Plate

Hemanth Dileep¹, Kaushal Kumar Jha², Pallab Sinha Mahapatra¹, Arvind Pattamatta^{1*}

¹Indian Institute of Technology Madras

Chennai, Tamil Nadu, India

²Center for Excellence in Energy and Telecommunication (CEET)

Chennai, Tamil Nadu, India

^{1*}arvindp@iitm.ac.in

Abstract - Effective thermal management is paramount in ensuring the optimal performance, longevity, and safety of Li-ion cells. This paper presents a comprehensive investigation into the thermal management of Li-ion batteries under extreme climatic conditions, focusing on a 20Ah cell. Experimental studies were conducted utilizing an infrared (IR) camera to analyse thermal behaviour at low discharge rates of 1C, 2C, and 3C in an environment with temperatures reaching 40°C. The region of elevated temperature within the cell corresponds closely to the terminals, as captured by the IR camera. Subsequently, a validated NTGK battery model was employed to predict temperature increases within the cell under higher discharge rates of 4C and 5C, resulting in maximum temperatures of 82°C and 92°C, respectively. Building upon insights gleaned from thermal images of the pouch cell, a novel localized cooling design, termed the T-shaped cold plate, was proposed. This innovative design demonstrated a remarkable reduction in maximum temperature rise during 5C discharge, achieving a substantial 31°C decrease. To further optimize this cooling system, the effects of inlet flow rates and coolant temperatures were explored. Results indicated that mass flow rate exerted negligible influence on maximum temperature rise, while lowering inlet coolant temperature led to reduced temperature elevation, albeit with a trade-off of increased non-uniform temperature gradients. Through systematic analysis, an inlet coolant temperature of 30°C emerged as the optimal choice, balancing maximum temperature mitigation and temperature uniformity considerations. Overall, the T-shaped cold plate offers mitigating thermal issues in Li-ion batteries under extreme environmental conditions, paving the way for lightweight and economical thermal management systems.

Keywords: Thermal management, Pouch cell, Infrared camera, NTGK model, T-shaped cold plate

1. Introduction

Over the past decade, the thermal management of Li-ion cells has surged in importance, primarily driven by the electrification trend in the automotive sector aimed at phasing out internal combustion engines. Li-ion battery chemistry stands out as the prime candidate for electric vehicle (EV) batteries, but it is highly sensitive to operating temperatures. The performance, ageing, and safety of Li-ion cells are profoundly influenced by temperature variations. Maintaining an optimal operating temperature range of 15-45°C, with a maximum temperature difference of 5°C within the cell, is crucial [1]. Pouch cells, known for their energy density, can experience significant temperature rises, leading to large temperature gradients within the cell. These gradients can cause local variations in the state of charge, negatively impacting cell performance [2]. Moreover, if the cell's temperature exceeds 85°C, it can trigger a catastrophic event known as thermal runaway, posing severe safety risks. Thus, effective thermal control of Li-ion cells is paramount for ensuring the longevity and safety of EVs. Given the non-uniform heat generation within the cell, its temperature distribution is typically non-isothermal, with higher temperatures often observed near the terminals. Consequently, cooling requirements on the cell surface are not uniform, necessitating the exploration of localized cooling strategies in battery thermal management. In addition to experimental approaches, numerical studies play a crucial role in battery thermal management research. These studies enable the prediction of scenarios that may be unsafe or prohibitively expensive to explore experimentally, such as thermal runaway or high discharge rates. The Newman, Tiedemann, Gu, and Kim (NTGK) model is widely employed due to its ability to accurately simulate battery behaviour with fewer model parameters [3]–[5]. Significant research efforts are underway to enhance the thermal management of EV batteries, utilizing various cooling methods, including air cooling, liquid cooling, phase-change material cooling, and heat pipe cooling [6]. Among these, liquid cooling is prevalent in many commercial electric vehicles, such as Tesla and Tata. Traditionally, cooling the entire battery surface has been a common practice, but this approach may result in over-cooling certain regions due to non-uniform temperature distribution. Alternatively, Verma et al. [7] investigated

the effectiveness of multiple minichannels arranged on the cell surface, observing a substantial decrease of 23°C in the volume average temperature compared to no cooling. In summary, advancements in thermal management techniques, including localized cooling strategies and numerical modelling, are essential for enhancing the performance, longevity, and safety of Li-ion batteries in electric vehicles.

This study investigates the thermal characteristics of a 20Ah pouch cell employing an innovative approach utilizing an Infrared (IR) camera, diverging from the conventional use of thermocouples prevalent in the existing literature. Experimental investigations are carried out under extreme ambient conditions of 40°C, initially focusing on low discharge rates. The Asian continent is increasingly experiencing extreme ambient temperatures of 35°C and above as a consequence of global warming. Consequently, it is imperative to thoroughly investigate the impact of these increased ambient temperatures on cells. Understanding these effects is crucial for the development of a resilient thermal management system. Subsequently, the scope is expanded to include high discharge rates of 4C and 5C, employing the NTGK model, which is validated against in-house experiments. By leveraging thermal imaging of the cell, areas of localized heating, or "hotspots," are identified. Based on these findings, a localized cooling plate is proposed. The study further delves into the analysis of the cooling plate's efficacy in mitigating thermal issues within the cell. This research not only provides valuable insights into the thermal behaviour of the 20Ah pouch cell but also introduces a practical solution for managing localized heating through innovative cooling strategies.

2. Experimental Methodology

The experimental setup comprises a thermal chamber, a battery charging-discharging unit (Neware 100A-5V), an infrared (IR) camera (FLIR A655sc), and the test cell, a 20Ah pouch cell from A123 systems. The schematic representation of this setup is provided in the Fig.1. The specifications of the cell are given in Table 1. The thermal chamber serves the function of regulating the ambient temperature surrounding the test cell. To enhance temperature measurement accuracy, the test cell is initially coated with matte black paint. This coating aids in precise and reliable temperature data acquisition by the IR camera. The battery charging-discharging unit is employed for controlling the discharging and charging processes of the test cell according to the desired C-rate. The IR camera captures the temperature distribution across the surface of the test cell. Operating at a capture rate of 1Hz, the IR camera provides surface temperature distribution essential for analysing temperature dynamics during the experiment. In this study, the cell undergoes discharging at rates of 1C, 2C, and 3C at an ambient temperature of 40°C. Throughout these experiments, the cell undergoes cooling only by natural convection within the thermal chamber.

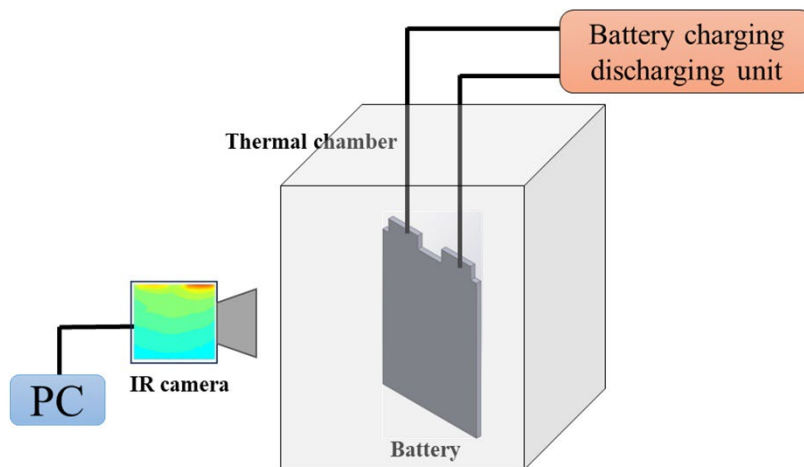


Fig. 1: Schematic of experimental setup

3. Numerical Methodology

The 3-dimensional computational domain of the cell is numerically modelled in ANSYS Fluent 21R. The NTGK model, model, a Multiscale Multidomain (MSMD) approach available in Fluent, is used for the electrochemical modelling of the the cell. The NTGK model first estimates the model parameters U and Y from the voltage vs time data at different C-rates rates generated from in-house experiments. The expressions for U and Y are given by,

$$U = \left(\sum_{n=0}^3 b_n \text{DoD}^n \right) - C_2(T - T_{\text{ref}}) \quad (1)$$

$$Y = \left(\sum_{n=0}^5 a_n \text{DoD}^n \right) \exp \left(-C_1 \left(\frac{1}{T} - \frac{1}{T_{\text{ref}}} \right) \right) \quad (2)$$

$$\text{DoD} = \frac{\text{Vol}}{3600 Q_{Ah}} \left(\int_0^t J dt \right) \quad (3)$$

Where C_1 and C_2 are battery constants, T is the temperature, DoD is the depth of discharge of the cell, Vol is the volume of the cell, and Q_{Ah} is the nominal capacity of the cell. The model parameters are used to calculate the volumetric current transfer rate (J),

$$J = aY(U - (\phi_+ - \phi_-)) \quad (4)$$

Where ϕ_+ and ϕ_- are the phase potentials at the positive and negative electrodes. Now, the governing equations for the electric and thermal fields are solved in the cell domain.

$$\nabla(\sigma_+ \phi_+) = -J \quad (5)$$

$$\nabla(\sigma_- \phi_-) = J \quad (6)$$

$$\dot{q} = J \left(U - (\phi_+ - \phi_-) - T \frac{dU}{dt} \right) + \sigma_+ \nabla^2 \phi_+ + \sigma_- \nabla^2 \phi_- \quad (7)$$

Where \dot{q} is the volumetric heat generation in the cell and σ_+ , σ_- are the electrical conductivities of positive and negative electrode. The energy equation (Eqn.7) is solved to get the temperature data in the cell. The cooling studies on the cell involve laminar incompressible flow with governing equations,

$$\nabla \cdot \vec{V} = 0 \quad (8)$$

$$\frac{\partial \vec{V}}{\partial t} + (\vec{V} \cdot \nabla) \vec{V} = -\frac{1}{\rho} \nabla P + \nu \nabla^2 \vec{V} \quad (9)$$

$$\frac{\partial T}{\partial t} + \nabla \cdot (\vec{V} T) = \alpha \nabla^2 T \quad (10)$$

Where, V is the velocity, P is the pressure, ν is the kinematic viscosity and α is the thermal diffusivity of the fluid. Cooling is achieved using water as the coolant. The pressure-based solver available in Fluent is used for the computational study of coolant flow. SIMPLE scheme is used for pressure-velocity coupling. PRESTO is used for pressure discretization.

The second-order upwind scheme is used for both momentum and energy discretization. Unsteady computations have been performed till a convergence of 10^{-6} is achieved at each time step for all conservation parameters. The thermo-physical properties used for simulations are given in the Table 2.

Table 1. Material properties used for simulation

Properties	Cell body	Positive tab	Negative tab	Coolant
Material	Active zone	Aluminum	Copper	Water
Density (kg/m ³)	1868	2719	8978	998
Thermal conductivity (W/m-K)	$k_x=18.6$ $k_y=5$ $k_z=0.5$	202	387.6	0.6
Specific heat (J/kg-K)	678	871	381	4182
Viscosity (Pa.S)	-	-	-	0.001003

3.1 Model validation

The computational domain has been discretized using structured hexahedral elements of three distinct sizes, namely 0.08, 0.15, and 0.3 million elements. The findings of the grid independence study are depicted in Fig. 2(a). With a maximum temperature error of 0.3% between the 0.15 million and 0.3 million mesh configurations for the cell discharged at 2C, the 0.15 million mesh is chosen for subsequent investigations to reduce computational cost. The experimental results of the temperature dynamics of the cell are compared with those predicted by the numerical model to check the reliability of the model. The Fig.2(b) shows the experimental and numerical results of maximum temperature rise in the cell for discharge rates of 1C, 2C and 3C at an ambient temperature of 40°C. The model shows a good agreement in predicting the maximum temperature rise within an error of 12%.

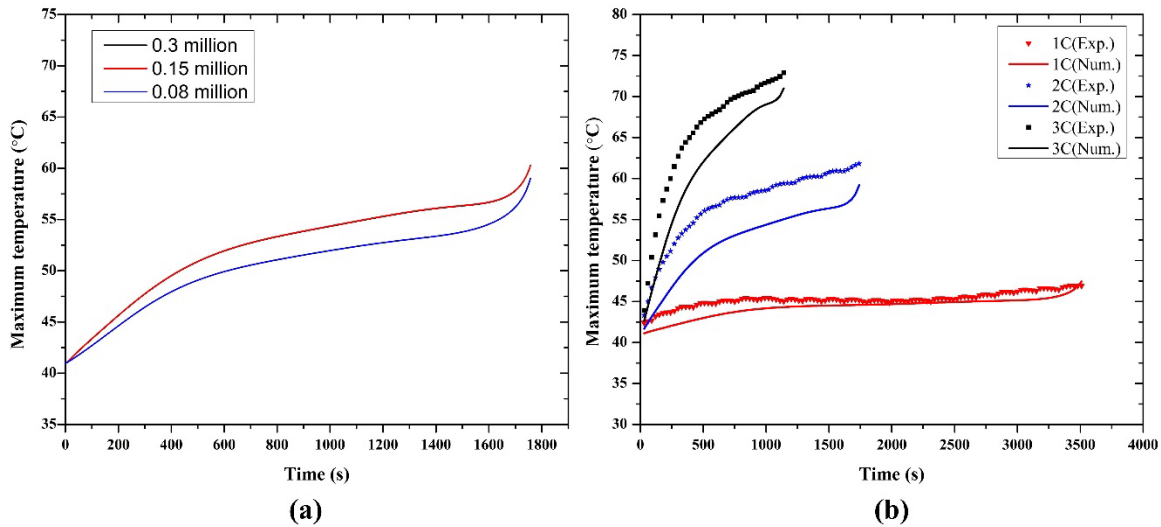


Fig. 2: (a) Grid Independency study, (b) Comparison between numerical and experimental results for 1C, 2C and 3C discharge rates

4. Results and Discussions

This study investigates the temperature behaviour of a 20Ah pouch cell under extreme conditions, specifically discharging at rates of 4C and 5C, with an ambient temperature of 40°C, employing numerical modelling. To mitigate potential thermal runaway risks, a T-cold plate is suggested to manage the maximum temperature increase within the cell.

4.1 Infrared temperature profiles of the cell during low discharge rates

The surface temperature profile of the pouch cell was examined using an infrared (IR) camera under varying discharge rates of 1C, 2C, and 3C, within an extreme ambient temperature of 40°C as shown in Fig.3. The resulting temperature distribution at the conclusion of discharge revealed a notable non-uniform pattern, with elevated temperature zones primarily concentrated near the tabs. Notably, the hottest spot was identified at the positive terminal. At the termination of discharge cycles, peak temperatures were recorded at 48°C, 62°C, and 73°C for the 1C, 2C and 3C discharge rates, respectively.

This data suggests that even at a discharge rate as moderate as 2C, the battery's temperature exceeded the recommended safe operational threshold for Li-ion cells, set at 60°C under 40°C ambient conditions. The detailed temperature distribution observed through IR imaging provides valuable insights into the cooling requirements of the cell. Notably, a distinct temperature gradient was observed, with approximately 30% of the top surface, particularly around the terminal sides, exhibiting significantly higher temperatures compared to the remainder of the battery surface. Additionally, it was observed that the central region of the battery tended to be hotter than its sides. Furthermore, the IR thermography revealed a distinct pattern of heat propagation, indicating that heat waves emanated from the terminal sides and propagated across the entire battery surface. This information underscores the importance of localized cooling strategies to mitigate temperature differentials and ensure uniform thermal management across the cell. Hence, a T-shaped cold plate design is proposed, and its cooling performance is discussed in the following sections.

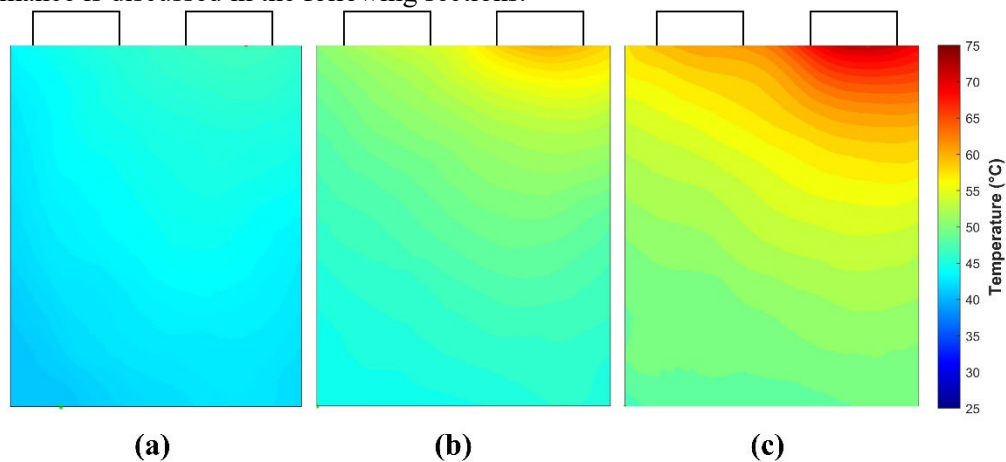


Fig. 3: Infrared temperature profiles (postprocessed in MATLAB) at the end of discharge: (a) 1C, (b) 2C and (c) 3C

4.2 Temperature characteristics of the cell at high discharge rates

Given that the cell experienced temperatures nearing 73°C at a discharge rate of 3C, it's deemed unsafe to experimentally test the cell at discharge rates exceeding 3C due to the elevated risk of thermal runaway. However, real-world scenarios may entail higher discharge rates, necessitating numerical modelling for analysis. Utilizing the NTGK MSMD model, the temperature dynamics of 4C and 5C discharge rates at a 40°C ambient temperature were investigated. Fig.4 depicts the maximum temperature increases observed during discharge at 4C and 5C rates. At the end of 4C and 5C discharge rates, the maximum temperatures recorded within the cell were 82°C and 92°C, respectively. These temperatures are significantly concerning for the health of the Li-ion cell, particularly considering that temperatures exceeding 80°C are recognized as the threshold for initiating thermal runaway. It's evident that higher discharge rates, coupled with elevated ambient temperatures, pose a grave risk to the life and safety of the cell. Consequently, the implementation of an efficient thermal management system becomes imperative to mitigate such risks and ensure the cell's stable operation under extreme conditions.

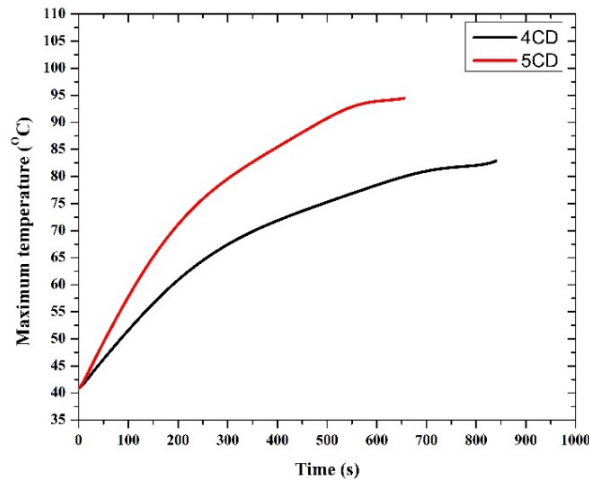


Fig. 4: Temperature profile predicted by model for 4C and 5C discharge rates at 40°C ambient

4.3 Performance of T-cold plate at higher discharge rates

Departing from the conventional approach of cooling the entire cell surface, a localized cooling design is proposed in this section. A T-shaped cold plate designs having cooling surface area of 40% of cell surface is introduced, and its cooling capabilities under extreme conditions, specifically 5C discharge at 40°C, is evaluated. The schematics of the T-shaped cold plate design is depicted in the Fig 5(a). The T-shaped cold plate features a T-junction, where coolant is introduced through the horizontal faces and exits through a common vertical outlet. The mass flow rate of 0.02kg/s and an inlet temperature of 25°C are taken as the flow conditions for comparison. The transient rise of maximum temperature for cells subjected to natural convection and T-cold plate design is illustrated in the Fig.5(b). Remarkably, T cold plate design effectively mitigate the maximum temperature rise within the cell, capping it at below 60°C which is the safe operating temperature limit for the Li-ion cells. This enhanced cooling is attributed to the horizontal and vertical component of the T-cold plate, which facilitates efficient heat dissipation from the regions near to the terminals and central region of the cell, thereby containing temperature rise towards the other uncooled cell surface. Due to its pronounced cooling efficiency and ability to effectively manage temperature distribution within the cell, the T-cold plate is selected for further investigation and analysis.

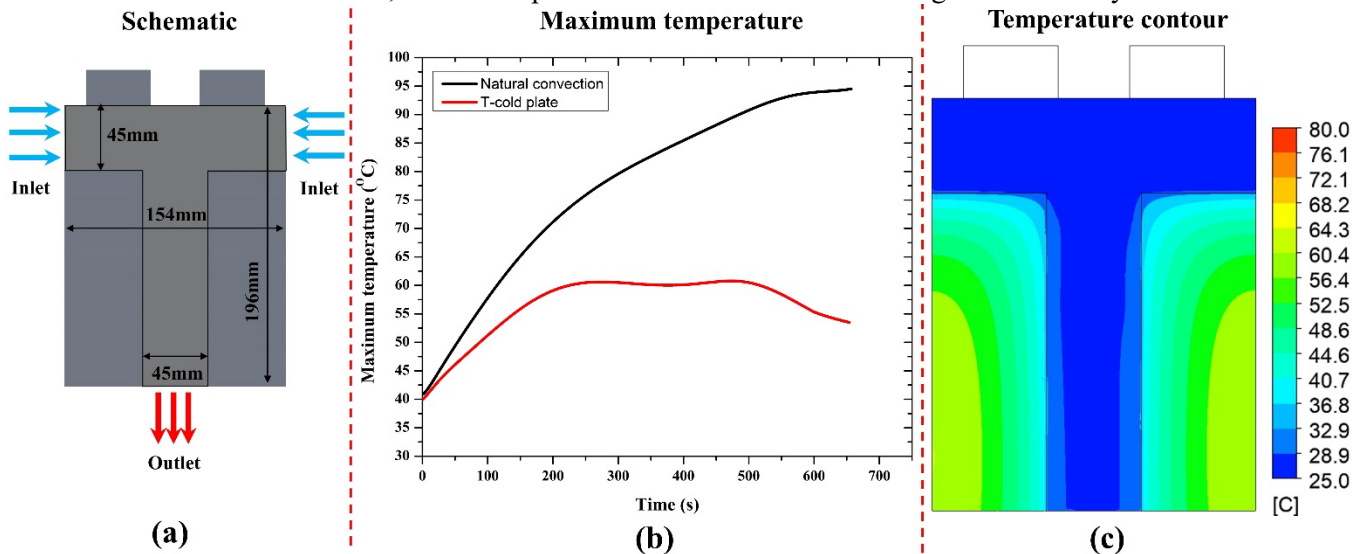


Fig. 5: (a) Schematic of T-cold plate, (b) Maximum temperature rise during 5C discharge, (c) Numerical temperature contour of the cell with T-cold plate

Furthermore, the Fig.6 illustrates the influence of coolant mass flow rate at a constant inlet temperature of 25°C. It is observed that varying the mass flow rate within the tested range doesn't significantly impact the maximum temperature. With the T-cold plate, the maximum temperature decreases by approximately 30°C for both discharge rates, prompting the selection of the lowest mass flow rate (0.02kg/s) for subsequent investigations. The impact of inlet coolant temperature on maximum temperature rise is then examined, considering three temperatures: 25°C, 30°C, and 35°C as shown in Fig.7(a) and (b). At a discharge rate of 4C, the lowest maximum temperature of 52°C is recorded for a coolant temperature of 25°C, while the highest of 56°C is noted for 35°C inlet temperature. Similarly, for a discharge rate of 5C, the trend persists, with the lowest maximum cell temperature of 62°C at 25°C and the highest of 65°C at 35°C. Lowering the coolant temperature effectively reduces the maximum cell temperature; however, it also introduces more temperature non-uniformity across the cell surface. The Fig.7(c) illustrates the maximum temperature difference on the cell surface under 5C discharge at various inlet temperatures. Notably, coolant with an inlet temperature of 35°C exhibits less temperature non-uniformity compared to that with a 25°C-inlet temperature. This disparity arises from the intense localized cooling provided by the cold plate, which effectively cools regions in direct contact with the cell but less so for regions farther away. Consequently, excessively reducing the coolant inlet temperature beyond a certain threshold is deemed unfavourable for battery thermal management due to the resulting high-temperature gradient induced within the cell. Hence, under 40°C ambient temperature, 30°C is found to be the best inlet coolant temperature.

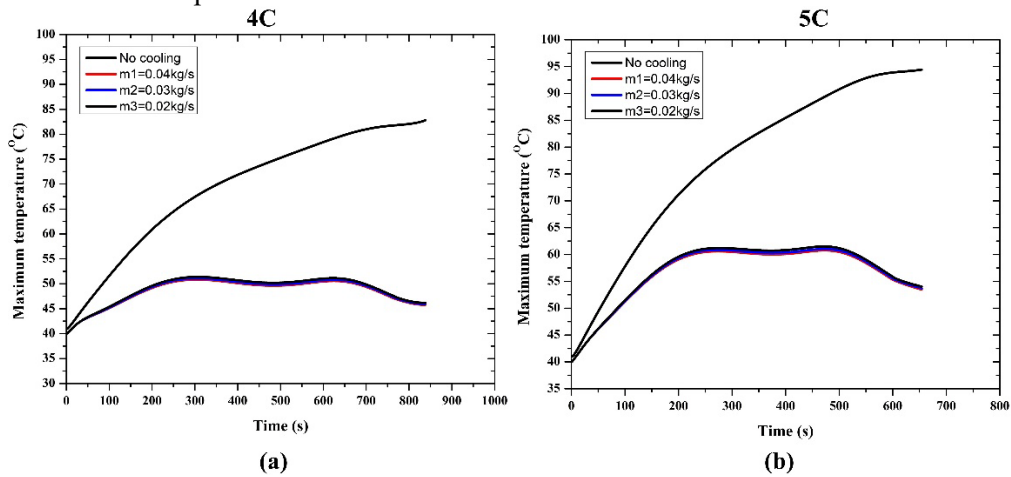


Fig. 6: Effect of mass flow rate for T-cold plate: (a) 4C and (b) 5C discharge rates at 40°C ambient

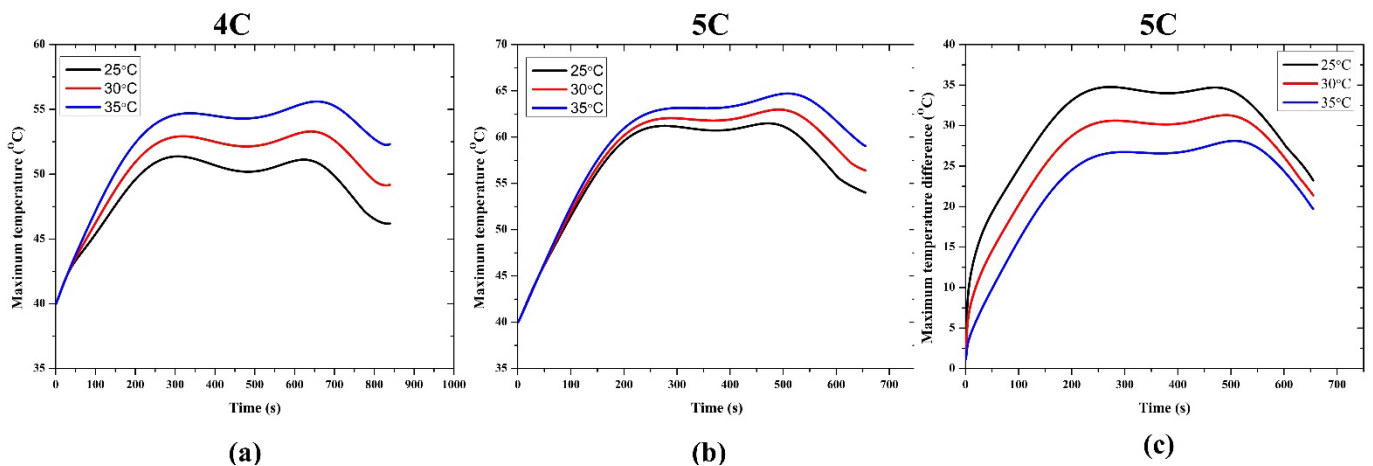


Fig. 7: Effect of coolant inlet temperature for T-cold plate: (a) 4C and (b) 5C discharge rates, (c) Maximum temperature difference for 5C discharge rate

4. Conclusion

The major conclusions from the present study are:

- Experiments were conducted on a 20Ah cell, assessing low discharge rates of 1C, 2C, and 3C, with temperature measurements facilitated by an IR camera at an ambient temperature of 40°C. Notably, discharging at a 3C rate resulted in a peak temperature of 73°C at discharge completion.
- Utilizing a validated NTGK model, forecasts were made for maximum temperature elevations at higher discharge rates of 4C and 5C, projecting temperatures of 82°C and 92°C, respectively.
- Leveraging insights from Infrared thermography, a proposed localized T-shaped cold plate design demonstrated a substantial reduction in maximum temperature rise, achieving a decrease of 31°C during 5C discharge via liquid cooling with an inlet coolant temperature of 25°C.
- Examination of the mass flow rate's impact on the cell's maximum temperature rise revealed negligible effects. Considering both maximum temperature rise and temperature non-uniformity on the cell, a coolant temperature of 30°C was identified as optimal under 40°C ambient conditions.

Acknowledgements

The first author acknowledges the Prime Minister Research Fellowship (PMRF) by the Government of India

References

- [1] A. Pesaran, "Battery Pack Thermal Design", [Online]. Available: <https://www.osti.gov/biblio/1304580>
- [2] M. Klein, S. Tong, and J. W. Park, "In-plane nonuniform temperature effects on the performance of a large-format lithium-ion pouch cell," *Appl. Energy*, vol. 165, pp. 639–647, 2016, doi: 10.1016/j.apenergy.2015.11.090.
- [3] M. Suresh Patil, J. H. Seo, and M. Y. Lee, "A novel dielectric fluid immersion cooling technology for Li-ion battery thermal management," *Energy Convers. Manag.*, vol. 229, no. November 2020, 2021, doi: 10.1016/j.enconman.2020.113715.
- [4] A. Adeniran and S. Park, "Optimized cooling and thermal analysis of lithium-ion pouch cell under fast charging cycles for electric vehicles," *J. Energy Storage*, vol. 68, no. April, p. 107580, 2023, doi: 10.1016/j.est.2023.107580.
- [5] Luo, L., Liao, Z., Wang, Z., Liu, Y., Zhong, J., Hong, X., Ai, P. and Wu, W, "Investigation of the heat generation characteristics of lithium-ion battery and orthogonal analysis of its constructal cold plate structure parameters," *Case Stud. Therm. Eng.*, vol. 52, no. July, p. 103750, 2023, doi: 10.1016/j.csite.2023.103750.
- [6] J. Kim, J. Oh, and H. Lee, "Review on battery thermal management system for electric vehicles," *Applied Thermal Engineering*, vol. 149. Elsevier Ltd, pp. 192–212, Feb. 25, 2019. doi: 10.1016/j.applthermaleng.2018.12.020.
- [7] A. Verma, T. Saikia, P. Saikia, D. Rakshit, and C. E. Ugalde-Loo, "Thermal performance analysis and experimental verification of lithium-ion batteries for electric vehicle applications through optimized inclined mini-channels," *Appl. Energy*, vol. 335, no. October 2022, p. 120743, 2023, doi: 10.1016/j.apenergy.2023.120743.